CHAPTER 3

SWAMP AND LACUSTRINE DEPOSITS OF THE LAKE WANUM AREA

Lake Wanum, centred on 6°38'S and 146°47'E, lies about 25 km inland from the Huon Gulf on the southern flank of the Markham Valley. It has an irregular outline and, with a maximum width of about 3 km, is the largest of a number of lakes and swamps in the vicinity. The area consists predominantly of granodiorite, extensively faulted in the upper Quaternary, which gives rise to a topography of steep slopes with rounded ridges and flat bottomed valleys. Various small swamps and lakes are found at the foot of these hills some possibly being impounded by faults (Chappell, 1973).

To the west of Lake Wanum over a narrow fault scarp lie the Erom-Erom lakes (Plate 3.1), a series of three small ponds and associated swamps. More extensive swamps and at least two other lakes are found bounding the hills to the west and south of the area. To the south-east on the edge of the granodiorite is the large expanse of Redhill Swamp (Fig. 3.1).

The Lake Wanum basin itself appears to be delimited by at least two major fault lines, along the northern and western shores. To the east the marginal hills are less steep in the immediate vicinity of the lake. The bathymetric sketch map[1] (Fig. 3.2) shows a similar trend continuing under water, the deepest part of the basin (19 m below datum) occurring near the steeply sloping northern shore.

---

[1] Compiled from echo-sounding traverses made by Joe Glucksman of the Fisheries Research Division of D.A.S.F. and the author in August 1974.

FIGURE 3.1. The distribution of lakes and swamps in the Lake Wanum area

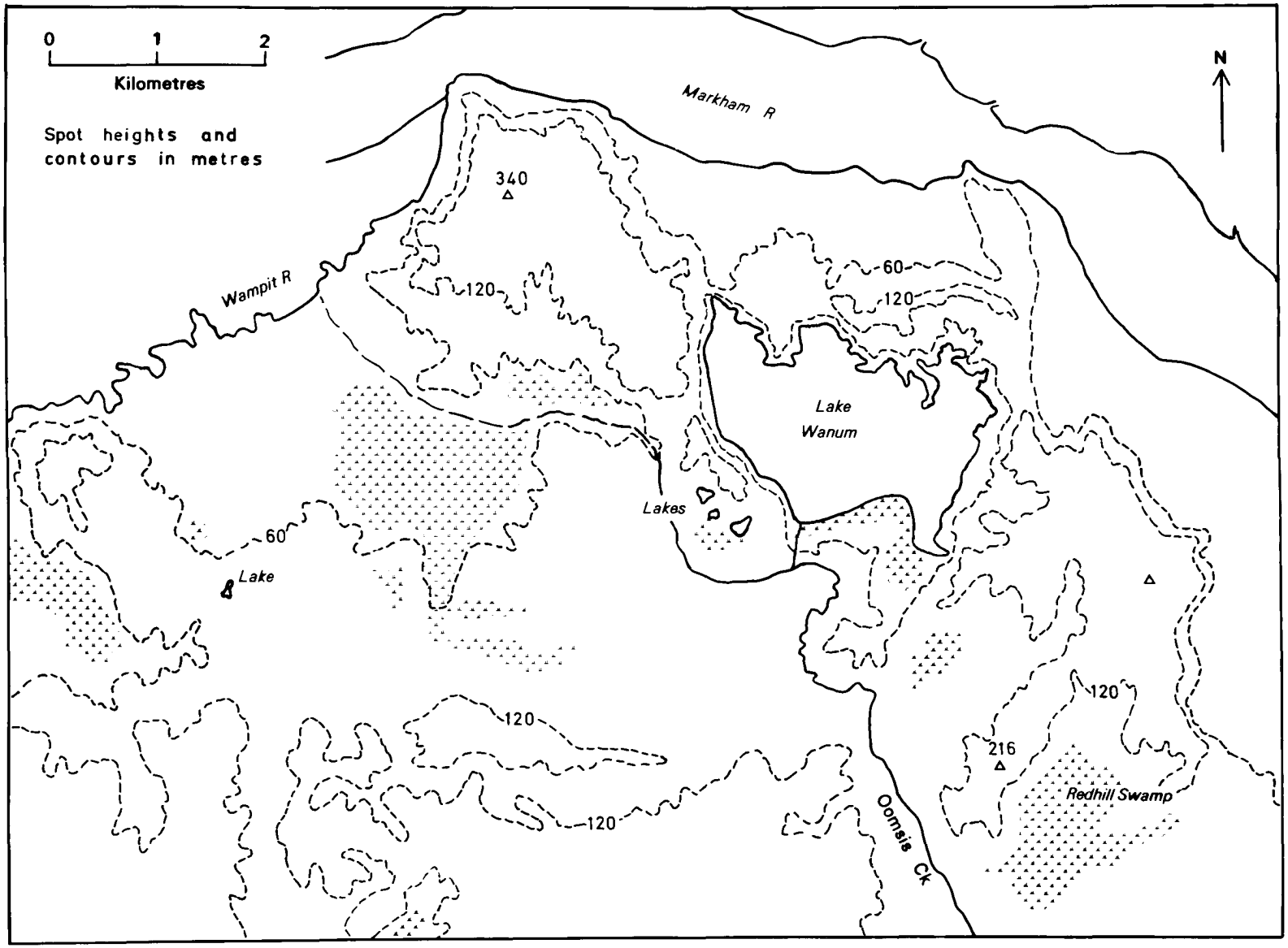

FIGURE 3.2. Lake Wanum: Bathymetric sketch map. Underwater contours are in metres

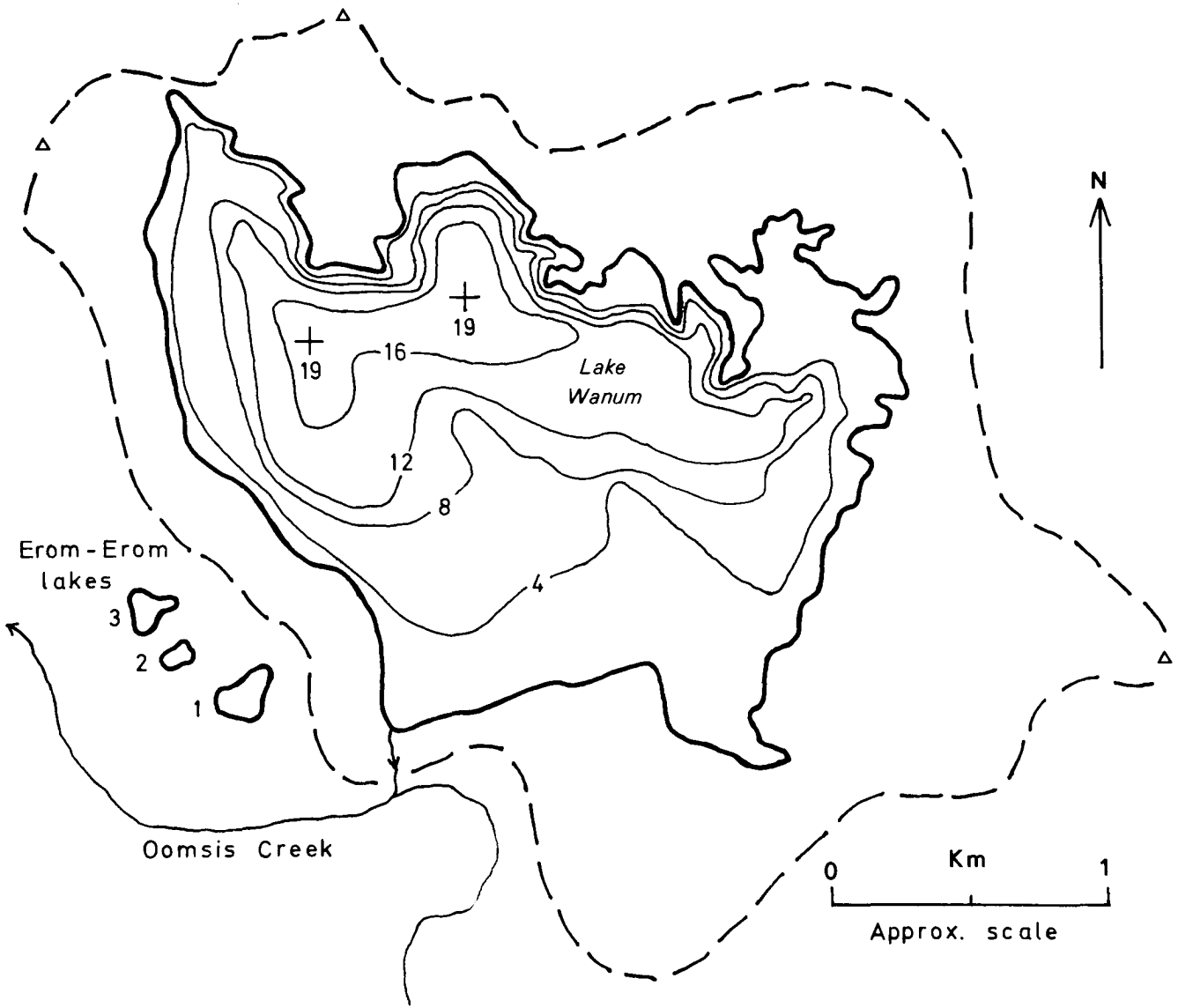

PLATE 3.1 The Erom-Erom lakes and Lake Wanum, an oblique aerial view from the south-west. The course of Oomsis Creek is marked by riparian forest in the foreground, and the Markham River is visible in the distance.

PLATE 3.2. The eastern shore of Lake Wanum, an oblique aerial view from the north. Several islands of herbaceous swamp vegetation are visible in the north-east bay.

The area of open water in the basin, about 3.7 km^2, is fairly large in relation to the total catchment area of approximately 8 km^2 as measured from the map. As there is no permanent stream inflow into the lake much of its water must be derived by precipitation directly onto the lake surface, and the water is fresh and clear. The only outflow of the lake is a small channel in the extreme south-west corner of the basin that runs into Oomsis Creek. This operates only intermittently. It was observed flowing throughout the latter half of 1974, but had dried up and become overgrown by May 1976 when the lake level was apparently slightly lower. Brass (1964) reports that this channel also serves as an inflow when the creek is in flood. Oomsis Creek is the only more or less permanent watercourse in this locality although Brass also reports that it too may cease flowing under conditions of sustained dry weather.

The altitude of the water surface of Lake Wanum above sea level is not known accurately. The 1944 1:63 360 map[1] shows it as between 150 feet and 200 feet (45 to 60 m). Using the heights of nearby hills given on this map as a basis, a crude triangulation with an Abney level determined the lake surface as 34 m or 36 m above sea level. If the height for Mt. Ngaroneno given on the 1966 1:250 000 map[2] ($\pm$ 340 m) is taken as correct, the lake level becomes 16 m above sea level. A similar exercise at Erom-Erom lake 2, shown on the 1 inch map as between 250 feet and 300 feet (60 to 75 m) produced figures of 41 m or 23 m for the lake surface depending on the datum height used.

---

[1] No. 0452 Nadzab 1 inch series.
[2] SB 55-10 Markham sheet.

STRATIGRAPHIC INVESTIGATIONS

Coring techniques

In the recovery of sediment cores for stratigraphic description the primary equipment used was a version of the Livingstone-Vallentyne stationary-piston corer incorporating the modifications of Walker (1964). The sampler was operated from a small, flat bottomed, aluminium dinghy provided with a central coring hole. This apparatus proved successful in obtaining cores of reasonable length when firmly anchored in shallow water. In open water deeper than about 5 m stable anchorage of the boat became a problem and cores longer than *c.* 4 m were difficult to obtain. Instability was overcome by positioning the boat, or subsequently a 2 m x 2 m plywood coring platform, on top of islands of floating or loosely rooted vegetation. In this way cores over 20 m in depth were recovered.

During 1976 a compact pneumatically operated corer (Mackereth, 1969) was employed to obtain cores up to 1 m long with an undisturbed sediment/water interface. The 'mini-Mackereth' was successful in recovering both a core of highly cohesive sediment from the deepest part of Lake Wanum, and cores of the uppermost sections of the highly unconsolidated marginal sediments.

All cores were extruded in the field. Those collected solely for stratigraphic description were discarded after examination. Others were sealed in polythene sheeting, and enclosed in PVC pipe for return to Canberra.

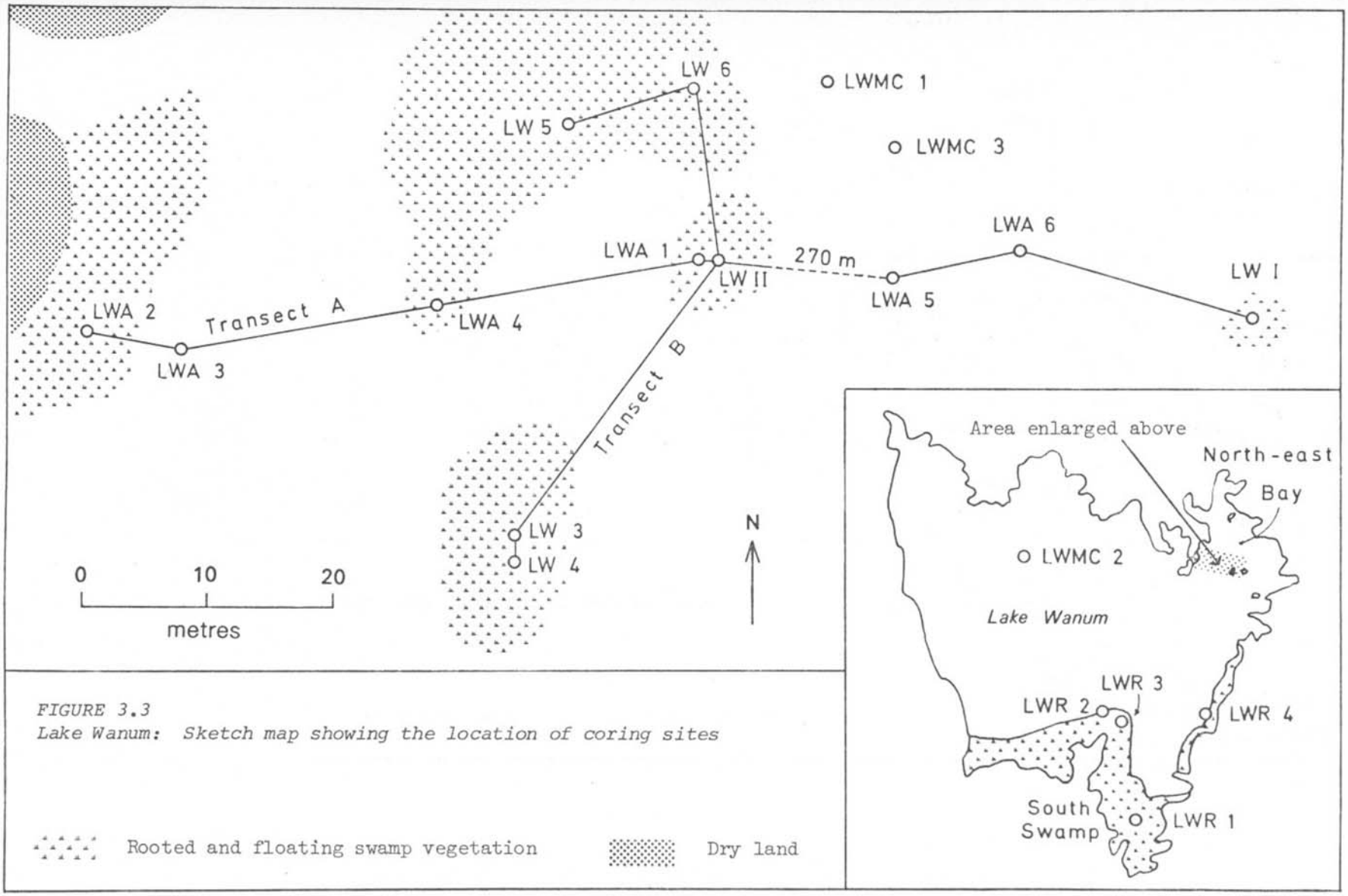

FIGURE 3.3
Lake Wanum: Sketch map showing the location of coring sites

FIGURE 3.4. Key to stratigraphic diagrams

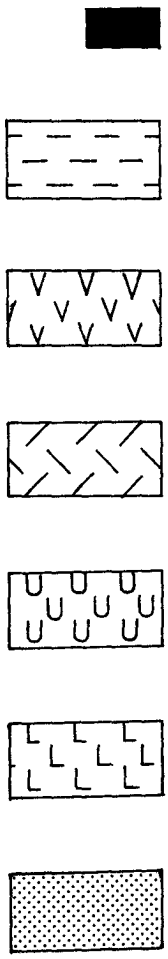

Location of radiocarbon dated sample

Substantia humosa (Sh)

Turfa lignosa (Tl) *and/or* Detritus lignosus (Dl)

Turfa herbacea (Th) *and/or* Detritus herbosus (Dh)

Limus calcareus (Lc)

Argilla steatodes (As)

Grana arenosa (Ga)

Major components only are shown in the stratigraphic column. Where two major components occur in a single horizon, both are drawn. Apart from the symbol for Grana arenosa, *superimposed at the true stratigraphic depth, alternation of symbols within a horizon is diagrammatic only. Minor components of the deposit are identified by abbreviations at the side of the column. Narrow discrete horizons are located by a dashed line, and identified adjacent to the column. The top of each stratigraphic column represents the sediment/water interface.*

FIGURE 3.5. Redhill Swamp: Stratigraphy of cores RHA 1 and RHB 1

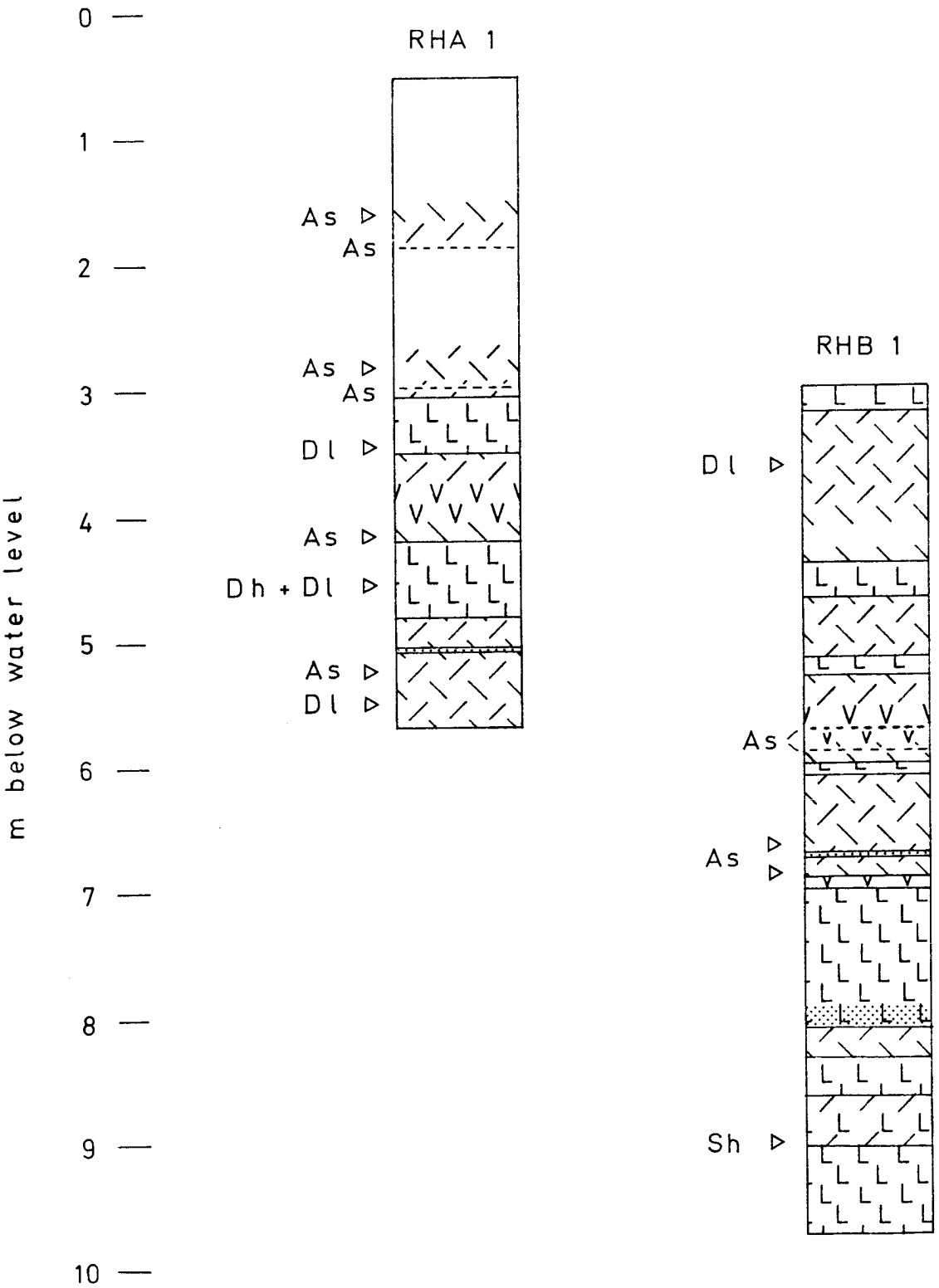

Description of deposits

In describing the characteristics and stratigraphy of the sediments the system of Troels-Smith (1955) is adhered to as far as practicable. Assessment of the physical properties and humicity of the deposits proved straightforward although recording of the generic terms used in the description of component elements of the deposit was less satisfactory. Many of Troels-Smith's more specialised terms are not applicable outside N.W. Europe, the region for which they were originally devised. Even the broader generic terms such as *Turfa, Detritus,* and *Limus* could not always be used with certainty as they imply a familiarity with the source of any macroscopic vegetal remains. These uncertainties are reflected in the use of alternative terms for the same horizon, or in the case of highly humified deposits use of the purely descriptive term *Substantia humosa*. As a further aid to the interpretation of the stratigraphy, a subjective description of the deposits is also given. The symbolic representation of various deposit types (Fig. 3.4) is a simplified version of Troels-Smith's system.

The stratigraphy of Redhill Swamp

Coring was carried out in the Lake Wanum area during two field seasons both in the basin of the lake itself (Fig. 3.3), and in the large Redhill Swamp to the south.

Two reconnaissance cores were taken near the south-eastern margin of Redhill Swamp: RHA1 located about 100 m from the edge of the swamp, and RHB1, approximately 200 m from dry land. The generalised stratigraphy of these cores is shown in Fig. 3.5. Both show a succession of grey clay (*Argilla steatodes*) bands,

intercalated with predominantly organic bands of fibrous peat (*Turfa herbacea*) often including horizons of wood or woody fragments. Although both sequences contain a similar range of deposits, the stratigraphy is complex, and detailed correlation is not possible.

Passage through the swamp was extremely difficult. The water depth was too great to proceed on foot, and the dense herbaceous vegetation and frequent presence of small saplings made movement with the boat very slow. The stratigraphy suggested that the marginal areas of the swamp would be unlikely to provide any cores with a long, continuous sedimentation record. Therefore, subsequent efforts to obtain such cores for pollen analytical purposes were concentrated in the basin of Lake Wanum itself.

The stratigraphy of Lake Wanum

Four reconnaissance boreholes (LWR 1 to 4) were cored in the large area of herbaceous swamp and open water vegetation, the 'south swamp', bounding the southern shore of Lake Wanum. In addition, a number of probes to determine the depth of sediments was made using the corer extension rods alone. In LWR 1 to 3 a cohesive grey plastic clay (*Argilla steatodes*) was found to underlie a shallow horizon (max. thickness 10 cm) of poorly humified fibrous organic deposit (*Turfa herbacea*). The clay was penetrated to a depth of *c*. 80 cm before its cohesive nature arrested the corer, precluding the recovery of any deeper sediments. Core LWR 4 shows a similar stratigraphy, although dark, gritty organic layers are also present. The numerous probes suggested that the thick clay layer was widespread over the whole southern area of the lake basin.

TABLE 3.1. Stratigraphic description of core LW II

Depth of horizon (cm below datum)	Colour	Structure and General Description	Troels-Smith Indices: *Nigror*	*Elasticitas*	*Siccitas*	*Humositas*	Component Elements	Radiocarbon Samples (cm below datum)
0-*c.* 200		Water and unconsolidated floating root-mat	-	-	-	-		
c. 200-600		Water	-	-	-	-		
600-685	Light brown	Fibrous organic sediment, slightly humified. Upper portion very wet. (No sample 600-635 cm)	2	2	1-2	1-2	*Turfa herbacea (Th)*	645-652+ 653-660 (ANU-1570)
685-800	Light brown/ grey	A heterogenous horizon of fibrous organic material admixed with grey inorganic clay. Gradual transition into the underlying horizon.	1-2	2	2	2	*Th* + *Argilla steatodes (As)*	775-790 (ANU-1688)
800-925	Brown	Well humified, slightly fibrous organic deposit.(No sample 900-906 cm).	2	2	2	3	*Th*	923-930+ 931-938
925-1000	Reddish-brown	Course fibrous organic deposit, wetter and less humified than the overlying horizon. Many well preserved rootlets present. Grades into underlying horizon.	2	4	2	2	*Th*	(ANU-1646)
1000-1080	Brown	Well humified organic deposit with some macroscopic plant fragments including rootlets and leaves. Fragments of yellow wood are found between 1023-1033 cm.	2	2	2	3	*?Th+Turfa lignosa (Tl)* or *Detritus lignosus (Dl)*	
1080-1115	Olive-brown	Similar to above horizon. Fine rootlets present, with woody rootlet and wood fragments between 1083-1088 cm. Gradual change into underlying horizon.	2	2	2	3	*Th + Tl*	
1115-1191	Brown	A fibrous organic horizon, although well humified, and becoming more so towards the base. In the upper part some wood and large leaves are present, penetrated by both large and fine rootlets. A solid band of light coloured wood occurs at 1188-1191 cm.	2	3	2	3	*Th+Tl* and possibly *Detritus herbosus (Dh)*	1123-1130+ 1131-1138 (ANU-1718)
1191-1346	Dark brown	A well humified horizon with fewer macroscopic organic remains. Some fine rootlets are present between 1191-1199 cm, with both fine and larger rootlets between 1219-1269 cm. Wood fragments occur from 1261-1269 cm. Between 1269-1280 cm, the deposit becomes slightly more humified and darker in colour. Large intact pieces of yellow wood are present around 1300 cm. From 1300-1346 cm scattered wood, rootlets and leaves occur. (No sample 1280-1300 cm).	3	2	2	3	*Th + Tl*	

TABLE 3.1. (Cont.)

Depth of horizon (cm below datum)	Colour	Structure and General Description	Troels-Smith Indices: *Nigror*	*Elasticitas*	*Siccitas*	*Humositas*	Component Elements	Radiocarbon Samples (cm below datum)
1346-1348	Light grey/ brown	A sharply defined band of grey clay, with some humified organic material and several large black fragments, possibly of carbonised wood.	1-2	0-1	3	-	*As* + *Substantia humosa (Sh)* + *Dl*	
1348-1463	Dark brown	Similar deposit to that between 1191-1346 cm, although slightly more humified. From about 1400-1430 cm the deposit becomes more fibrous, with some large rootlets. Towards the base, the colour becomes increasingly grey, with the inclusion of inorganic clay from the underlying horizon.	2-3	3	2-3	3	*Th* + *As*	1443-1450+1451-1458 (ANU-1719)
1463-1465	Grey/ brown	Fairly distinct band of plastic grey clay about 1.5 cm thick.	2	0-1	3	-	*As* + *Sh*	
1465-1487	Olive-brown/ grey	A heterogenous admixture of slightly fibrous organic sediment and grey clay. Inorganic content decreases towards the base.	2	1	3	3	*Th* or *Sh* + *As*	
1487-1488	Grey/ brown	Band of grey clay c. 1 cm in thickness.	2	0-1	3	3	*As* + *Sh*	
1488-1525	Black	Sharp boundary between overlying clay and this slightly fibrous, well humified organic layer. Some large and fine rootlets present. Gradual transition into underlying horizon.	3	3	3	3	*Sh* or *?Th*	
1525-1711	Olive-brown	A fine to coarse granular organic deposit, fibrous in places, with very few small rootlets. Fragments of light coloured wood occur around 1640-1643 cm.	2	2	3	3-4	*Dh* or *Detritus granosus (Dg)* + *?As*	1561-1570+1571-1580 (ANU-1689)
1711-1712	Orange brown	Sharp boundary between dark, almost matted organic deposit and a gritty sandy clay layer.	2	0	3-4	-	*?Th* + *Grana arenosa (Ga)* + ?some *As*	1711-1727 (ANU-1720)
1712-1755	Brown	Course organic deposit, though well humified. Noticably gritty, with some inclusions of orange-brown sand especially at 1725-1727 cm. Intact roots or twigs of light coloured wood occur at 1753 cm.	2	3	3	3	*Dh* + *Ga* + *?Dl*	

TABLE 3.1. (Cont.)

Depth of horizon (cm below datum)	Colour	Structure and General Description	Troels-Smith Indices: *Nigror*	*Elasticitas*	*Siccitas*	*Humositas*	Component Elements	Radiocarbon Samples (cm below datum)
1755-1770	Dark brown	Fine organic deposit with fairly sharp upper boundary. A few large rootlets occur. Slightly gritty in places. Gradual transition into underlying horizon.	2-3	2	3	4	*Th* + *Sh* + *Ga*	
1770-1862	Reddish-brown	Very fibrous organic deposit with many large rootlets. A diffuse clay band is visible around 1799 cm, and the deposit is slightly gritty in places especially at *c.* 1800 *cm*. Gradual transition into underlying horizon.	2	3-4	3	2-3	*Th* + *As* + *Ga*	1782-1790+1791-1799 (ANU-1810)
1862-1881	Brown-grey	Fibrous organic deposit admixed with clay.	2	3	3	3	*Th* + *As*	1865-1870+1871-1880 (ANU-1645)
1881-1888	Orange/grey-brown	Fairly abrupt transition into a compact, very gritty sand/clay layer. Lower limit of this horizon more diffuse.	2	0	3	-	*Ga* + *As* + *Sh*	1888-1890+1891-1902 (ANU-1644)
1888-1981	Dark brown	Fibrous organic deposit. Many ?cyperaceous leaves, and some rootlet penetration. Wood fragments occur at 1890 cm and between 1909-1912 cm.	3	3	3	3	*Th* + *Dh* + *?Dl*	1960-1970+1971-1979 (ANU-1586)

FIGURE 3.6. Lake Wanum: Stratigraphy of cores in north-east bay Transect A

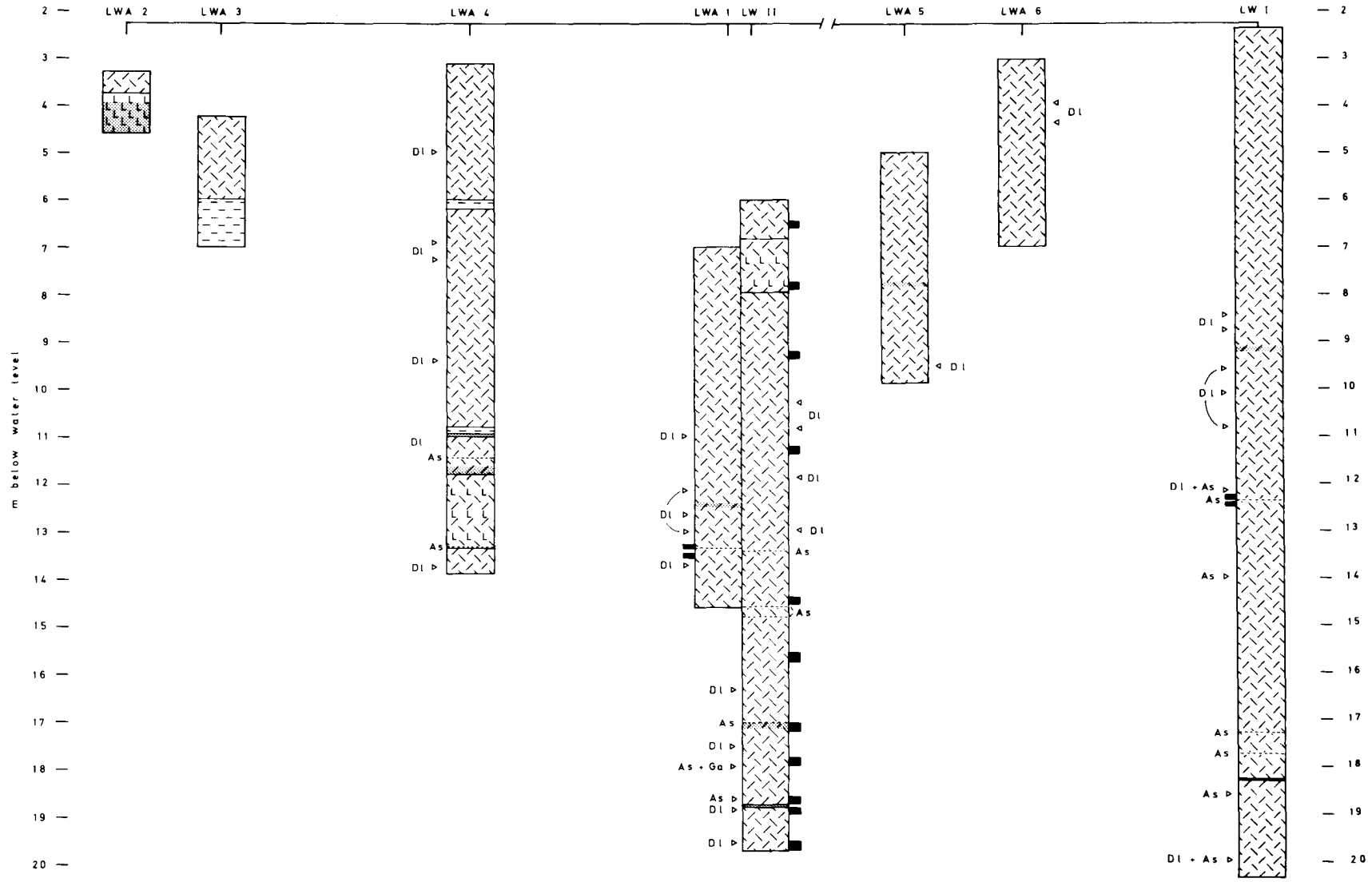

FIGURE 3.7. Lake Wanum: Stratigraphy of cores in north-east bay Transect B

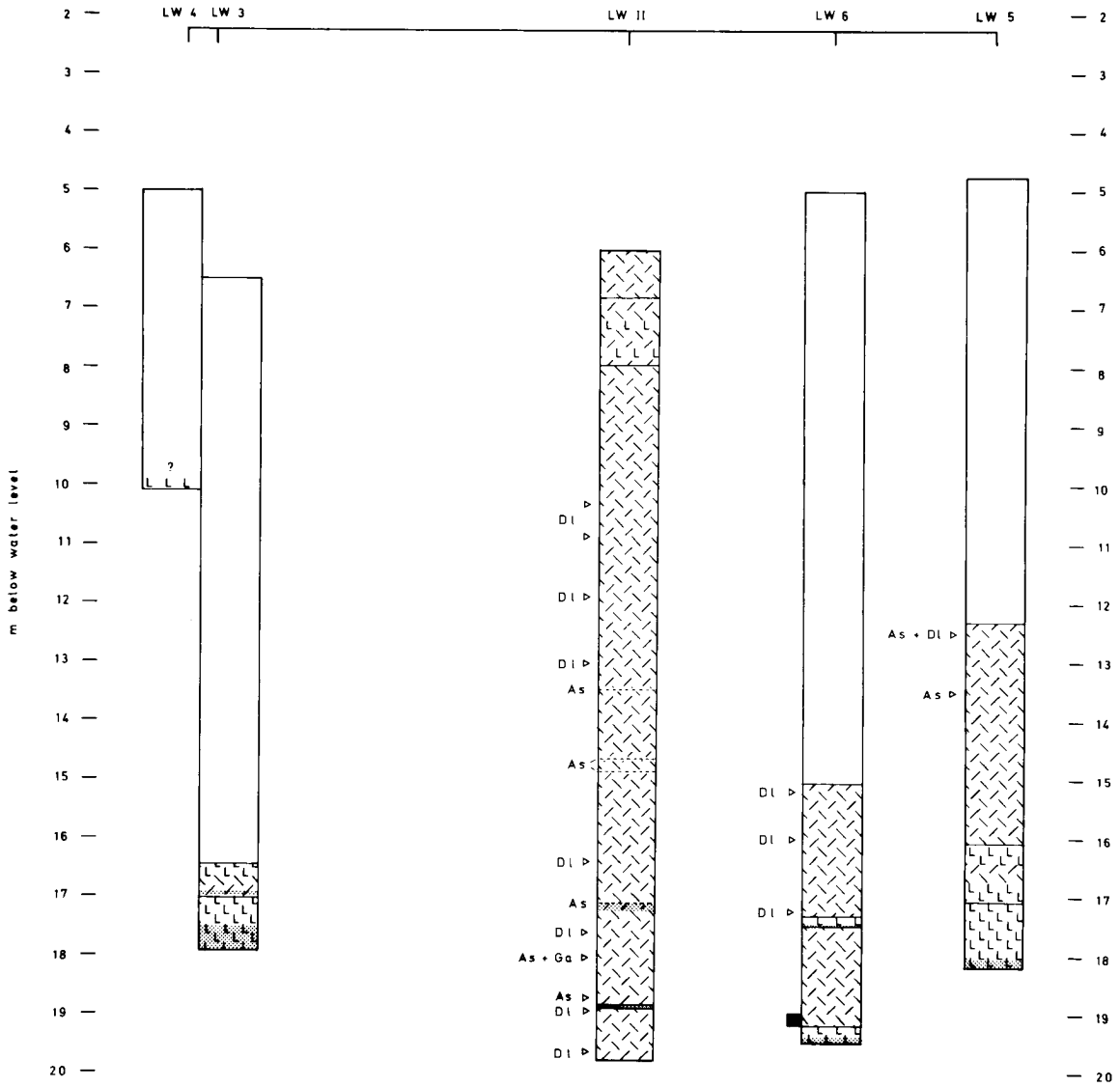

Subsequent investigations revealed the area of shallow water and sparse intermittent swamp vegetation at the north-eastern corner of the lake, (the 'north-east bay') to contain much deeper deposits of predominantly organic sediment. Probes at several locations away from the shore reached 14 m below water level (the maximum length of rods available at the time) without encountering substantial clay bands, or harder basal sediments. The major part of the stratigraphic survey was therefore concentrated in this area (Plate 3.2).

Although some shorter cores were recovered from open-water situations the location of coring sites (shown in Fig. 3.3) was largely dictated by the presence of suitable floating vegetation to act as a relatively stable base for operations. Hence the coverage of the coring transects is not as wide as is perhaps desirable, being largely restricted to a marginal area of swamp at the western edge of the bay, and a small area in the centre of the bay.

Of the cores in transect A recovered in 1974 two, LW I and LW II, were returned to the laboratory. Further cores were taken along the line of transect B in 1976 in order to elucidate the basal stratigraphy. All except LW 4 were retained for subsequent analyses. A detailed stratigraphic description of core LW II, selected for pollen analysis, is given in Table 3.1 whilst a generalised representation of the stratigraphy of the other north-east bay cores is shown in Figs. 3.6 and 3.7.

The longer cores show a generally similar, fairly uniform stratigraphy. The major component throughout most of the sequence is a fibrous organic deposit (*Turfa herbacea*) consisting

primarily of the roots and aerial stems of herbaceous swamp plants. In the upper sections of the cores this deposit is unconsolidated and poorly humified. At lower levels there is increasing occurrence of more strongly humified sediment, and in places very few macroscopic plant fragments are preserved.

The sequence of organic sedimentation is punctuated at intervals by bands, usually narrow, of plastic clay (*Argilla steatodes*), gritty clay, or sand (*Grana arenosa*). Most of these layers probably represent sediments derived by inwash from the lake shore, as they are more common in cores nearer the present water's edge. Inorganic bands also occur more frequently in the lower sections of the long cores than in the upper part. At least three cores (LW 3, 5 and 6) reach a substantial layer of plastic grey clay, sometimes admixed with a fine organic deposit, that grades into a compact gritty clay. This basal clay is presumably a decomposition product of the underlying granodiorite. Neither of the two longest cores (LW I and LW II) contacted this layer, the depth of recovery in these cases being governed by the limitations of the available coring equipment.

The basal stratigraphy suggests that the line of transect A from sites LWA 1 to LW II runs parallel to a relatively steep sided depression. Not only does the basal gritty clay occur closer to the surface towards the present shoreline, but also to the north and south of the transect line in the cores of transect B.

The two short cores LWMC 1 and LWMC 3 obtained from the north-east bay with the 'mini-Mackereth' corer show a stratigraphy similar to that found at the top of the longer cores. A shallow

layer of dark brown unconsolidated organic detritus (*Detritus granosus*) is underlain by a lighter brown fibrous deposit of rootlets and other poorly humified remains of swamp vegetation (*Turfa herbacea*).

In contrast, short core LWMC 2, from under *c.* 19 m of water in the deepest part of the lake basin, consists of very different sediments. A layer of fine, predominantly organic, mud (*Limus detritosus*) grades into a more clay-rich layer containing scattered fragments of leaves of swamp plants, wood, and well humified organic material. The proportion of plastic grey clay (*Argilla steatodes*) increases until it becomes the sole constituent towards the base of the 90 cm core.

ANALYSIS OF ORGANIC CONTENT

During the sampling of core LW II for pollen analysis, 71 sub-samples, each of approximately 3.9 ml, were set aside for determination of organic and inorganic content by estimate of weight loss on ignition. In order to relate this value to an appropriate gravimetric base the weighed samples were first dried in an oven at *c.* 100 ^{o}C, and the dry weight found. Each was then transferred to a crucible and ignited at 650 ^{o}C in an electric furnace for about 30 minutes. The residual ash was weighed and the loss on ignition calculated. This method, although less accurate than chemical titration methods is able to give an approximate value for the quantities of organic and inorganic sediment in most types of deposit.

The water content as a percentage of the wet weight, and loss of weight on ignition as a percentage of the dry weight, are shown in Fig. 3.8. The dry weight of the inorganic and organic

fractions per ml of wet sediment is shown in Fig. 3.9. As suggested by the stratigraphic description the sediments are very wet, containing typically 90% to 95% water. A slightly lower proportion of water is found in the predominantly inorganic layers. The curve for percentage residue after ignition ('inorganic' fraction) shows generally consistent trends, with several distinct 'peaks'. All of these can be related to stratigraphic horizons previously described (Table 3.1) as containing some proportion of *Argilla steatodes* or *Grana arenosa*. This curve, and the one based on the dry weight per ml (Fig. 3.9a) which is very similar, give a better quantitative indication of the inorganic component than that obtained from the stratigraphic description alone.

The weight loss on ignition ('organic' fraction) curve (Fig. 3.9b) shows few sustained trends. The values fluctuate considerably around the mean, although there is a tendency for the fluctuations to be of smaller amplitude below about 13 m in the core. This large variation in the organic content between adjacent samples could be the result of a number of factors. However, it is unlikely that errors in weight estimation are involved to any great extent, since the consistent curve for the organic fraction frequently relies on even lower values. Inaccurate collection of the volumetric sample could account for some of the variation since the unconsolidated, often fibrous, sediment found particularly in the upper part of the core is difficult to measure precisely. Nevertheless, it is likely that a major proportion of the observed variation is actually due to short-term fluctuations in sedimentation rate of the loosely compacted heterogenous organic material. This aspect will be discussed further in relation to annual sediment accumulation and pollen deposition rates.

FIGURE 3.8. Lake Wanum core LW II: Water content and weight loss on ignition

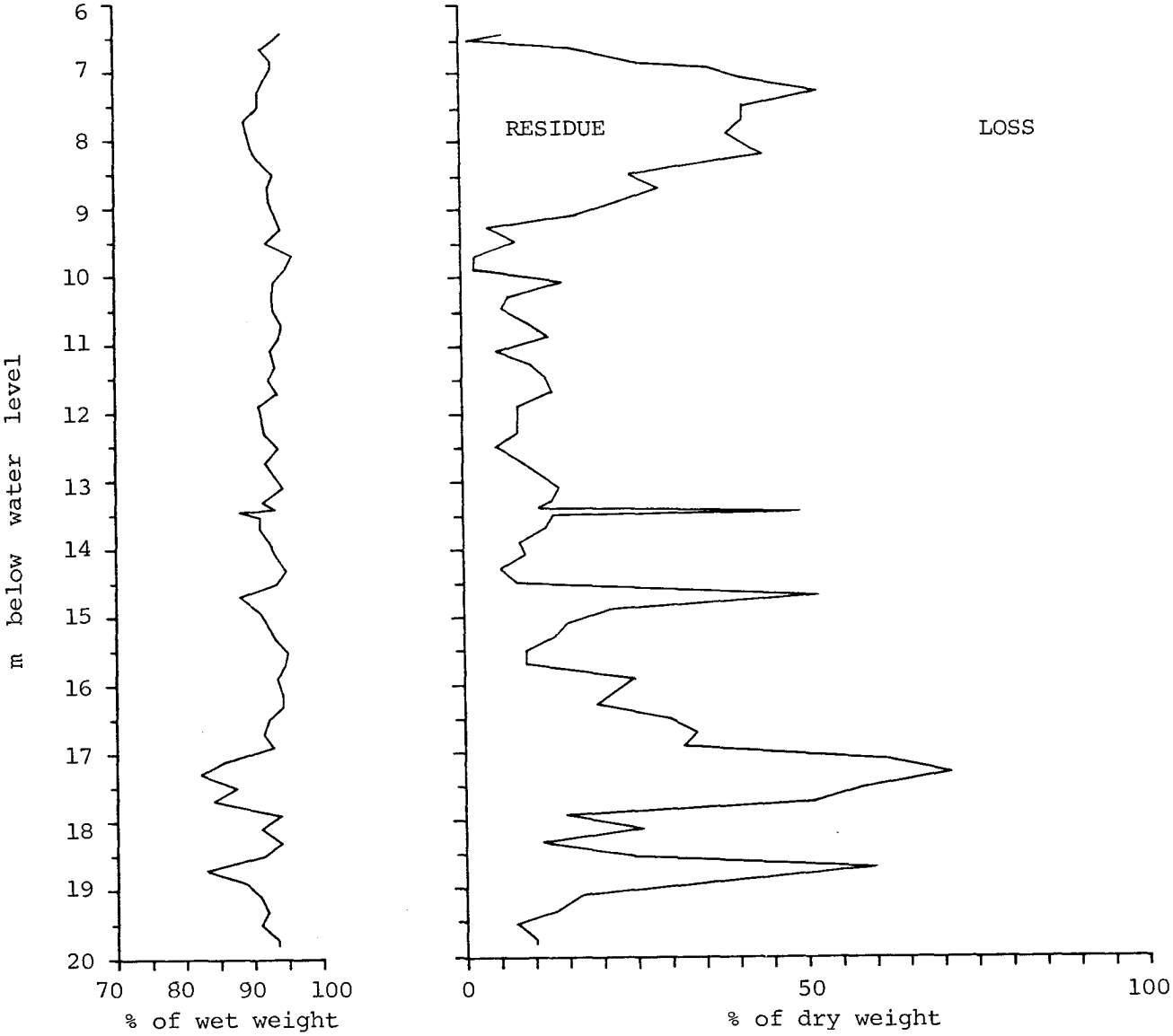

FIGURE 3.9. Lake Wanum core LW II: Sediment density for residue- ('inorganic') and loss-on-ignition ('organic') fractions

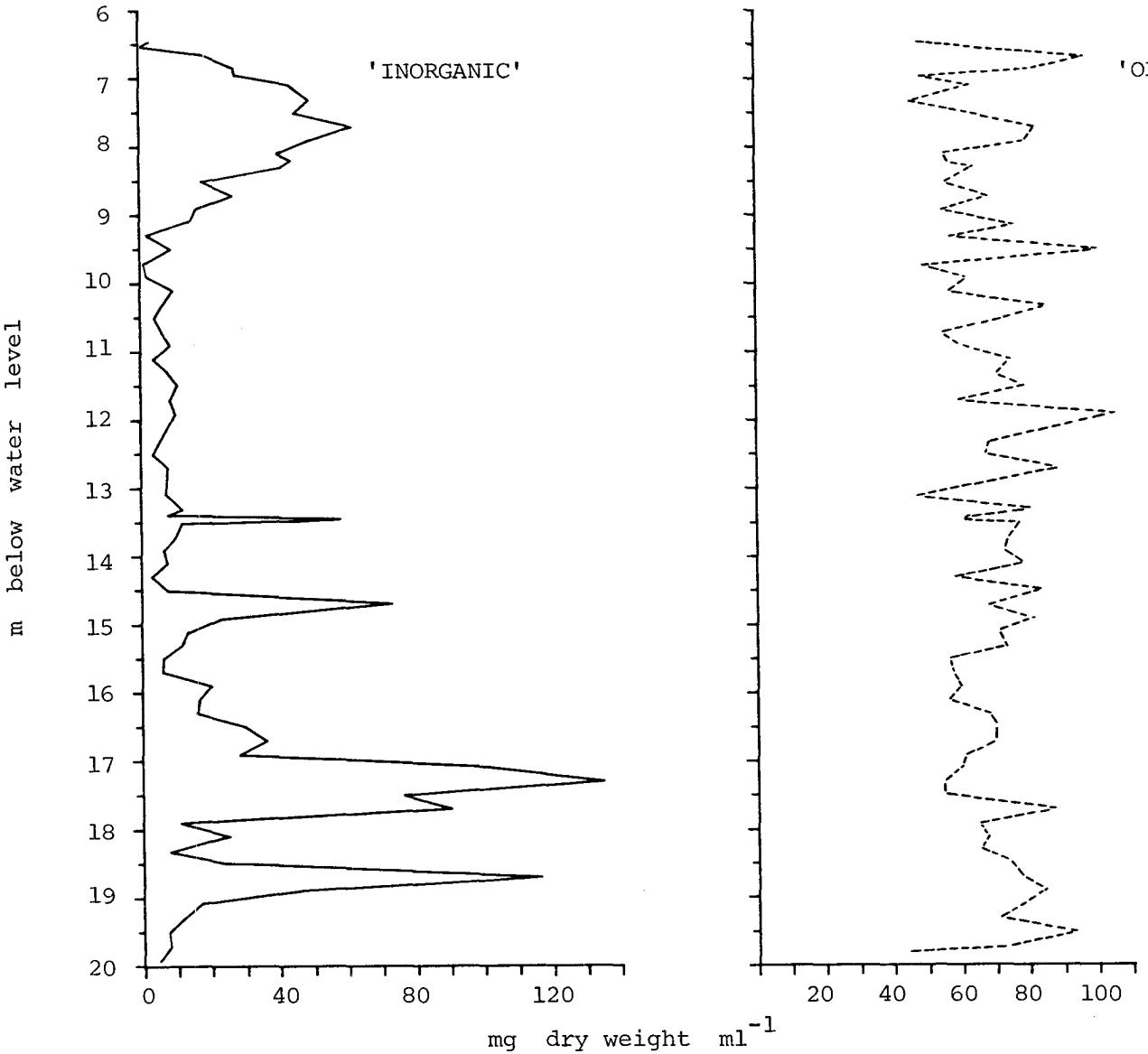

TABLE 3.2. Radiocarbon determinations from Lake Wanum

Core	Depth (cm below datum)	Lab. no.	Date ± 1 S.D.
LW II	645- 652 + 653- 660	ANU-1570	260 ± 60
LW II	775- 790	ANU-1688	1260 ± 100
LW II	923- 930 + 931- 938	ANU-1646	2070 ± 80
LW II	1123-1130 + 1131-1138	ANU-1718	3360 ± 80
LW II	1443-1450 + 1451-1458	ANU-1719	4290 ± 90
LW II	1561-1570 + 1571-1580	ANU-1689	4990 ± 100
LW II	1711-1727	ANU-1720	5480 ± 100
LW II	1782-1790 + 1791-1799	ANU-1810	6480 ± 100
LW II	1865-1870 + 1871-1880	ANU-1645	7740 ± 120
LW II	1888-1890 + 1891-1902	ANU-1644	8140 ± 130
LW II	1960-1970 + 1971-1979	ANU-1586	9400 ± 120
LWA 1	1330-1340	ANU-1447	3820 ± 90
LWA 1	1350-1360	ANU-1446	4040 ± 100
LW 6	1900-1908 + 1910-1918	ANU-1826	9550 ± 120
LW I	1225-1235	ANU-1449	2070 ± 130
LW I	1240-1250	ANU-1448	2710 ± 110

CORRELATION AND DATING

Detailed cross-correlation between cores on the basis of lithology alone is not straightforward, due to the general similarity of the organic deposits. Most of the predominantly inorganic layers, although readily discernable in individual cores can only be correlated with similar horizons in adjacent or nearby cores. The junction of the basal clay and the overlying organic deposits, whilst a distinct stratigraphic boundary, is not necessarily synchronous in all cores.

Palaeomagnetically based correlation

In an attempt to establish correlations between the near-basal sediments of the north-east bay, three cores from transect B (LW 3, LW 5 and LW 6) were subjected to magnetic analysis. The intensity of the horizontal component of the natural remanent magnetisation (NRM) and the magnetic declination of the intact cores were measured on a computerised slow-speed spinner magnetometer similar to that described by Molyneux *et al.* (1972). The peaks in NRM intensity generally correspond with inorganic layers in the deposits, whereas the predominantly organic sediments show a very low level of magnetic intensity. The basal gritty clay gives a reading between that of the smooth plastic clay and the organic deposits. This may be due to the acquisition by the clay of a degree of chemical remanence on weathering. It is interesting to compare this result with that from the deep water core LWMC 2. The clay in this core shows a very high NRM intensity, which together with its smooth homogenous nature suggest that it does not represent the basal clay horizon found in the other cores analysed.

Apart from this difference, the NRM results fail to discriminate between the inorganic horizons and do not assist greatly with stratigraphic correlation.

Dating

In order to provide an absolute chronology for the sedimentary history of the lake basin, an independent method of dating was required. The highly organic deposits proved very suitable for ^{14}C assay and a suite of sixteen determinations was provided by the ANU Radiocarbon Laboratory (Table 3.2). These dated samples, the location of which is indicated in Figs. 3.5 and 3.6, form the chronological basis of the stratigraphy of the north-east bay of Lake Wanum.

Due to the complex nature of the fine stratigraphy, and the marginal setting of the coring sites, the majority of the samples for dating were chosen from the core LW II. These served as a check on the continuity of sedimentation in the core, and provided a basis for the accurate assessment of sedimentation rate during the period of deposition.

The few dates obtained from other cores serve to emphasise the problems of correlation based solely on stratigraphy. A date of 2070 $\pm$ 130 (ANU-1449) which immediately overlies a narrow but distinct clay band in core LW I can be correlated directly with a similar date of 2070 $\pm$ 80 (ANU-1646) from core LW II, some 300 m distant, where no trace of the inorganic horizon is visible. Even between cores less than 25 m apart correlation of the fine stratigraphy is ambiguous. A satisfactory description of the three dimensional extent of the various sedimentary horizons in the north-east bay area would therefore seem to require a greater number of

closely spaced cores, or many more radiocarbon dates to substantiate possible correlations between the existing cores.

SWAMP DEVELOPMENT IN THE LAKE WANUM AREA

At this stage it is possible to advance a preliminary hypothesis in an attempt to explain the observed features of the sedimentary sequences and the present swamp distribution in the Lake Wanum area. This model will then serve as a testable framework for the subsequent accounts of sediment and pollen deposition rates, and of the evolution of the swamp vegetation.

Of the sediments recovered from the north-east bay of Lake Wanum, none are similar to the fine organic mud (*Limus detritosus*) accumulating today in the deeper part of the basin. In fact, many of the cores show sedimentary sequences in their lower portions which appear more similar to those found in the shallower water situation of Redhill Swamp. It is probable that most of the sediments of the north-east bay cores were formed in less than 10 m water depth. The base of the longer cores is on average 20 m below the present water surface. If the possible effects of subsidence and sediment compaction can be discounted, this in itself suggests a progressive increase in the water level of the lake basin, above that caused by sediment infill, during the period of the sedimentary record.

There are several ways in which such an increase could possibly occur. Firstly, given a totally enclosed basin, rise in water level could be achieved by increased effective precipitation or run-off, or a combination of the two. Alternatively in a basin with at least an intermittent outflow, such as is the current situation at Lake Wanum, impedance of this outflow by organic or

inorganic sedimentation could cause an increase in water level without any other change in the hydrological regime of the basin. There is perhaps some evidence for the second proposition in the topography of the lake basin, and the results of corings from the southern end of Lake Wanum. The extensive deposits of grey clay, overlain by only a thin band of organic material could be indicative of one or more episodes of inorganic deposition, presumably caused by overflow of the nearby Oomsis Creek. The presence of a similar horizon of grey clay, some of which incorporates detrital fragments of swamp vegetation, in a core from the deepest part of the lake basin could be seen as lending weight to this theory.

The hypothesis may be extended to explain the origin and distribution of other swamps and lakes in the area. The only available outflow from the Redhill Swamp basin is towards Oomsis Creek and the same situation occurs in the case of the Erom-Erom lakes, although here build-up of organic swamp sediments may also have assisted impedance of the drainage. A number of swamps are found in similar topographic locations between the hill slopes and the riparian or 'alluvium' forest of the creek area, particularly to the west of Lake Wanum.

The date of onset of organic deposition at these other swamps is largely a matter for conjecture, as the only radiocarbon dates come from the north-east bay of Lake Wanum. Here the base of the organic sediments give a date slightly older than 9500 BP. However, as this site is in a marginal area of the large lake, it is quite possible that onset of accumulation in deeper parts of the basin occurred earlier than this date.

FIGURE 3.10. Lake Wanum core LW II: Age/depth profiles for (a) uncorrected ^{14}C dates (±2 S.D.) and (b) recalibrated ^{14}C dates (±2 S.D.)

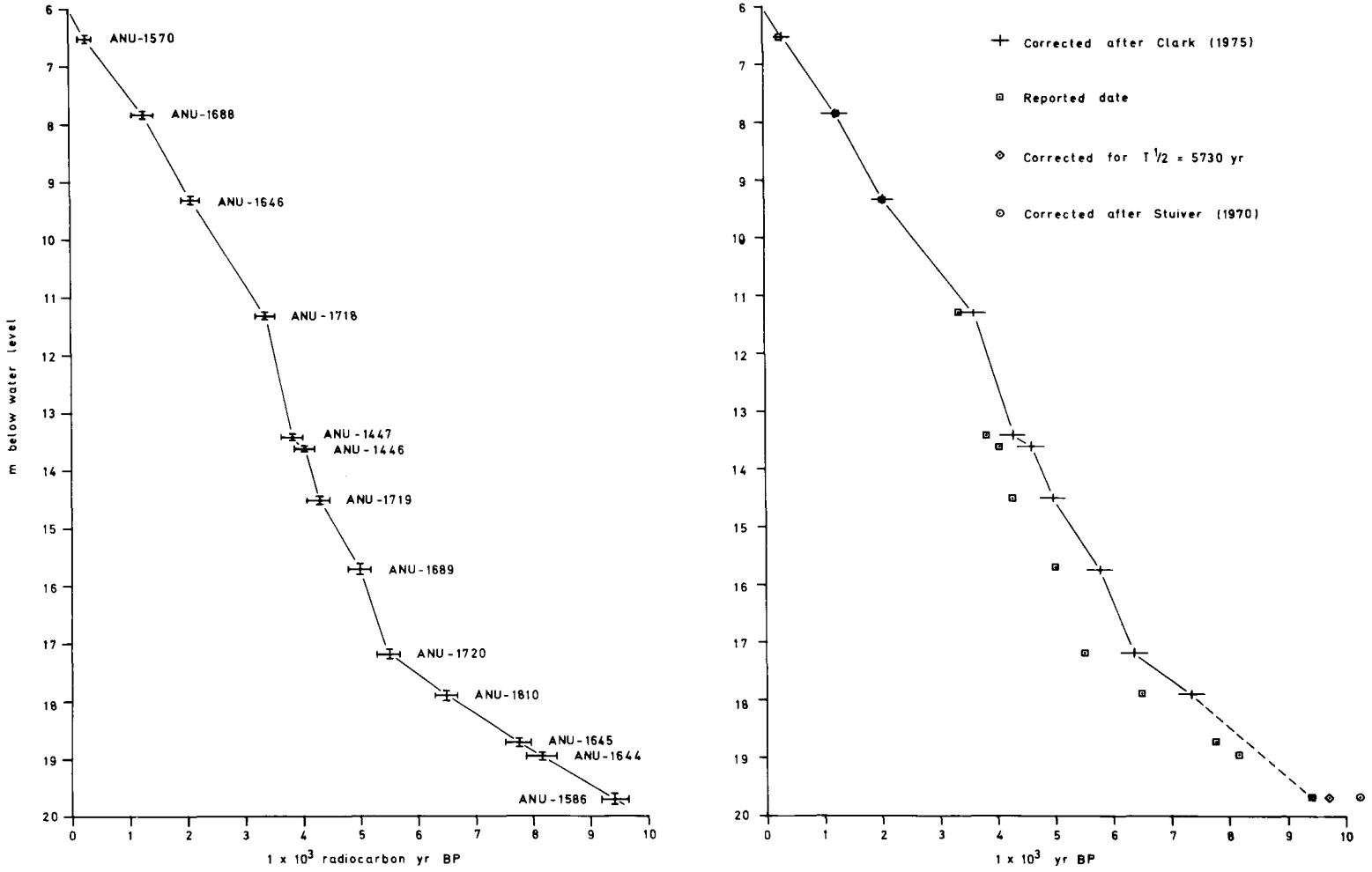

ESTIMATION OF ANNUAL SEDIMENT ACCUMULATION RATES

The radiocarbon chronology

The eleven radiocarbon dates from core LW II together with two correlated from an identifiable horizon in the adjacent LWA I core are shown plotted against depth in Fig. 3.10a. The physical mid-point of the sample is taken as the horizon to which the date refers. These determinations appear to provide a sound chronological basis for the estimation of annual rates of sediment and pollen deposition throughout the core. The dates follow the correct sequence, and there is no evidence of major discontinuities in sedimentation, or of any severe disturbance of the deposits. Neither is there any suggestion of a significant disequilibrium between the ^{14}C content of the sediments, and that of the atmosphere. Extrapolation of the rate of accumulation between the two uppermost dates to the diffuse sediment/water interface produces an apparent date close to the present. It can therefore only be assumed that a similar equilibrium has prevailed during the past.

Corrections to the radiocarbon timescale

Before attempting to construct the most appropriate sediment accumulation curve consistent with both the radiocarbon dates and the observed stratigraphy, it is necessary to consider certain limitations of the dating technique itself. These have been recently summarised by Olsson (1974) and Polach (1976).

By agreement, radiocarbon laboratories report dates as calculated on the basis of Libby's proposal of 5568 $\pm$ 30 years as the half-life ($T_{\frac{1}{2}}$) of ^{14}C (Libby, 1949). Strictly, such determinations should be corrected in line with the accepted revised

half-life of 5730 ± 30 years (Godwin, 1962). In practice this results in a small increase of about 3% in the reported age.

A more serious deviation from the absolute chronology is caused by lack of constancy, or secular variation, in the production rate of atmospheric ^{14}C over time. Long term increases in the production rate appear to occur in response to higher effective cosmic ray flux, perhaps due in part to decrease in the intensity of the geomagnetic field. This phenomenon was first observed by de Vries (1958), and its extent during the last 1200 years demonstrated by Willis *et al.* (1960) using a radiocarbon dated annual tree growth-ring sequence.

Subsequently a comprehensive tree-ring chronology has been constructed for the last 7500 years (Ferguson, 1970) using the wood from North American conifers *Pinus aristata* and *Sequoia gigantea*. Seuss (1967) produced the first calibration curve for the conversion of radiocarbon dates into 'absolute' ages, and his revised version (Suess, 1970) has been widely used. Several other correction curves or tables have also been produced from essentially the same tree-ring data, including those of Damon *et al.* (1972) and Ralph *et al.* (1973). The calibrations differ mainly in the degree of emphasis placed on small scale fluctuations in the atmospheric $^{14}C/^{12}C$ ratio, Suess's possessing the most 'wiggles' whilst that produced by Damon's group exhibiting only the longer term variations. Olsson (1974) synthesises these results by drawing a band covering 87% of the data points that she deems reliable.

The subjective method of obtaining the then existing calibration curves is criticised by Renfrew and Clark (1974) as being statistically unsatisfactory. As a result, Clark (1975) attempts to construct a curve using valid statistical techniques. He considers all the available data relating tree-ring ages to radiocarbon determinations, omitting over one-third not considered suitable for analysis. A calibration line is then derived using a curve fitting technique based on spline functions. The resulting curve is very similar to that drawn by Olsson (1974), but has the advantage of statistically defined confidence limits for the corrected ages.

No continuous radiocarbon dated dendrochronological sequence exists for the period before about 7500 years ago, although an extension of the existing chronology back to about 10 000 years ago is quite feasible (Ferguson, 1970). The information about atmospheric ^{14}C production beyond this date is therefore largely based on directly or indirectly dated varve sequences. The most comprehensive of these is the revised version of the Scandinavian varve chronology originally established by De Geer (1912) and discussed in relation to the radiocarbon time-scale by Tauber (1970). The chronology is dated indirectly by correlation of pollen zones between the lake sediments and nearby radiocarbon dated autochthonous deposits.

A sequence of varves from the Lake of the Clouds, northern Minnesota, U.S.A., counted by Craig (1972), has also been employed for calibration of the radiocarbon time-scale. The varved sediments, estimated to have been deposited over the last 9500 to 10 000 years, have been directly radiocarbon dated by Stuiver (1970).

Both varve chronologies imply atmospheric ^{14}C deviations for the period up to 7500 years similar to those shown by the dendrochronologically based curves. Beyond this age, however, the two sequences diverge. Tauber's curve shows a trend towards the datum (19th century AD ^{14}C production rate) until 8500 or 9000 varve years BP when the curve levels out, and uncorrected radiocarbon ages ($T_{\frac{1}{2}}$ = 5568) become almost synchronous with varve ages. A similar trend is shown by Stuiver's curve until about 8500 varve years ago, when the direction becomes reversed, and a continuing enrichment of atmospheric ^{14}C is indicated. The resulting discrepancy between the two chronologies thus becomes about 900 years at 10 000 varve years ago.

Whilst it is premature at this stage to accept either chronology as correct, the Scandinavian one does appear to be rigorously constructed, being derived from many geographically widespread varve sequences. Tauber's conclusions (Tauber, 1970) also appear to be supported by results from two other varve studies.

Vogel (1970) compares varve ages and radiocarbon dates from a Swiss site, using the varve chronology of Welten (1944). The trend in atmospheric ^{14}C concentration follows that postulated by Tauber until about 8500 BP. Prior to this date there appears to be a drastic reduction in ^{14}C production, which leads Vogel to cast doubts on the validity of the earlier section of the varve chronology.

A set of dated marine varves from Saanich Inlet, British Columbia, Canada (Yang and Fairhill, 1973), also produces results compatible with Tauber's. A decrease in atmospheric ^{14}C enrichment occurs until about 8500 varve years ago, values thereafter remaining close to the datum.

Such a trend may be supported by the theoretical models of Yang and Fairhill (1973), and Damon (1970). Fluctuations in the geomagnetic field intensity are assumed to follow a sinusoidal curve with a period of approximately 8000 years, peaking at about 2500 BP. The Saanich Inlet and Scandinavian results do not appear to confirm the theoretical increase in atmospheric ^{14}C concentration prior to about 9000 BP. This may be due to deficiencies in the model especially in relation to the time-lag in atmospheric response. This may not be constant, particularly if, as Damon (1970) suggests, the climatic influence on atmospheric ^{14}C levels may have been greater during the late Pleistocene period, than in more recent times.

The application of recalibrated radiocarbon dates

In order to investigate the possible effects of secular radiocarbon variation on the average accumulation rate from core LW II, the following corrections were applied. Dates younger than 6500 radiocarbon years BP were adjusted for the revised half-life and for secular variation using the calibration tables of Clark (1975). For recalibration of dates older than this, it was assumed that the rate of ^{14}C production in the atmosphere at about 9000 BP was similar to that of the 19th century AD datum. As the uncorrected dates lie in a relatively straight line, an age/depth curve for the period 7500 to 9500 calendar years BP was approximated by connecting the oldest dendrochronologically calibrated date (ANU-1810) to the oldest date (ANU-1586) by a straight line. Possible corrections to the basal date for the revised half-life of 5730 ± 40 years and the calibration suggested by Stuiver (1970) are also indicated (Fig. 3.10b).

TABLE 3.3. Comparison of average sedimentation rates of intervals between radiocarbon samples based on dates (A) as reported, and (B) corrected for revised half-life and secular variations

^{14}C sample interval	Mid-point of ^{14}C sample (mm)	Depth interval (mm)	A ^{14}C date ± 1 S.D. ($T_{½}$=5568)	A Time interval (^{14}C yr) ± 1 S.D.	A Average sedimentation rate, mm ^{14}C-yr^{-1} (± 1 S.D.) Min.	A Mean	A Max.	A mean. ^{14}C yr cm^{-1}	B Corrected date[a] ± 1 S.D.	B Time interval (yr) ± 1 S.D.	B Average sedimentation rate, mm ^{14}C-yr^{-1} (± 1 S.D.) Min.	B Mean	B Max.	B mean yr cm^{-1}	% difference of mean mm yr^{-1} from mean mm ^{14}C-yr^{-1}	
	6 000		- 25[b]						- 25[b]							
A_1		525		285 ± 60	1.52	1.84	2.33	5.43		359 ± 78	1.20	1.46	1.87	6.84	-20.7	A_1
	6 525		260 ± 60						344 ± 78							
A		1 300		1000 ± 117	1.16	1.30	1.47	7.69		903 ± 136	1.25	1.44	1.70	6.95	+10.8	A
	7 825		1260 ± 100						1237 ± 112							
B		1 480		810 ± 128	1.58	1.83	2.17	5.47		834 ± 147	1.51	1.77	2.15	5.64	- 3.3	B
	9 305		2070 ± 80						2071 ± 95							
C		2 000		1290 ± 113	1.43	1.55	1.70	6.45		1601 ± 148	1.14	1.25	1.38	8.01	-19.4	C
	11 305		3360 ± 80						3672 ± 113							
D		2 095		460 ± 120	3.61	4.55	6.16	2.20		615 ± 160	2.70	3.41	4.60	2.94	-25.1	D
	13 400		3820 ± 90						4287 ± 113							
E		200		220 ± 135	0.56	0.91	2.35	11.00		318 ± 163	0.26	0.63	1.29	15.90	-30.8	E
	13 600		4040 ± 100						4605 ± 117							
F		905		250 ± 135	2.35	3.62	7.87	2.76		363 ± 163	1.72	2.49	4.53	4.01	-31.2	F
	14 505		4290 ± 90						4968 ± 113							
G		1 200		700 ± 135	1.44	1.71	2.12	5.83		807 ± 165	1.23	1.49	1.87	6.73	-12.9	G
	15 705		4990 ± 100						5775 ± 117							
H		1 485		490 ± 141	2.35	3.03	4.26	3.30		571 ± 165	2.02	2.60	3.66	3.85	-14.2	H
	17 190		5480 ± 100						6346 ± 117							
I		715		1000 ± 141	0.63	0.72	0.83	13.99		993 ± 165	0.62	0.72	0.86	13.89	+ 0.1	I
	17 905		6480 ± 100						7339 ± 117							
J		820		1260 ± 156	0.58	0.65	0.74	15.37								
	18 725		7740 ± 120													
K		225		400 ± 177	0.39	0.56	1.01	17.78		2061 ± 168	0.80	0.87	0.95	11.51	+45.0	JKL
	18 950		8140 ± 130													
L		745		1260 ± 177	0.52	0.59	0.69	16.91								
	19 695		9400 ± 120						9400 ± 120[c]							

[a]Corrected dates derived from the calibration curve and tables of Clark (1975)
[b]Approximate top of sediment taken as 1975 A.D.
[c]Date as reported.

The average apparent sediment accumulation results derived from the original radiocarbon dates are compared with those produced using the recalibrated dates in Table 3.3. The effect of applying the calibrations is to produce differences in sediment accumulation rates of over 30% for some dating intervals within the tree-ring calibrated section, and of 45% in the less rigorously adjusted period before 6500 radiocarbon years BP. The average accumulation rates based on the uncorrected dates display greater variation than do those based on recalibrated dates. Maximum deviation of the two occurs between approximately 2000 and 4500 radiocarbon years BP, the period that sees the most rapid sustained increase in the rate of atmospheric ^{14}C production. This period also encompasses the fastest average accumulation rates in the core (dating intervals D and F) and under the corrected chronology these rates become reduced substantially. Conversely, between 6500 and 9600 radiocarbon years BP, if the declining trend of atmospheric ^{14}C production be accepted, the corrected average accumulation rate shows an increase of 45% over that implied by the original dates.

The general trend of atmospheric ^{14}C concentration over the past 7500 years is now well established, and is essentially synchronous and of the same extent over the globe. However, there still remain uncertainties as to the scale and direction of fluctuations before this date. In addition, the importance of changes in the ^{14}C production rate showing a shorter periodicity is yet to be resolved. It may be, as Olsson (1974) has proposed, that for samples thought to represent a small duration one should employ a calibration curve, such as Suess's, that emphasises these minor fluctuations. The radiocarbon samples analysed from Lake Wanum

variously represent time-spans of from about 60 to 300 years, depending on the prevailing accumulation rate. Short duration fluctuations would obviously influence the former samples to a greater extent than the latter.

Such unresolved problems in the application of radiocarbon calibration curves raise the question of the profitability of applying systematic corrections at all. The main constraint, in the current context, is the lack of an adequate calibration for the period prior to 6500 radiocarbon years ago. The trends in average sediment accumulation rate remain similar after application of the corrected dates, and there are no changes in the rate as great as an order of magnitude for any dating interval.

It was therefore decided to present the results of the sediment and pollen deposition studies on the basis of the reported radiocarbon ages alone, whilst taking into account the possible effects of gross secular variations in the interpretation. Thus all ages subsequently discussed in this thesis refer to uncorrected ($T_{\frac{1}{2}}$ = 5568) radiocarbon years BP (before present; 'present' = 1950 AD), unless indicated to the contrary.

The derivation of sediment accumulation rates

The reliability of an average sediment accumulation rate based on radiocarbon determination obviously depends on the frequency and magnitude of fluctuations in the true rate, and the number of dated horizons available. Given a series of dates, there is a number of ways in which a 'best fit' curve for the accumulation rate may be derived.

In a situation where the accumulation rate is thought to be essentially static, it may be possible to fit a simple regression line to the given dates. Thus Davis and Deevey (1964) used a least-squares regression line to produce an accumulation curve for the late-glacial section of their Rogers Lake core. Ogden (1967) attempted a similar method for two other north-eastern American lakes, but found standard deviations from the regression lines to be large, and his original assumptions 'too simple'. Maher (1972) also fitted a least-squares regression to dates from Redrock Lake, Colorado, and found a good linear correlation between age and depth. However, systematic deviations from the linear trend, probably caused by increasing compaction of the older deposits, could be best explained by fitting a power (log-log) function to the data. Using a polynomial regression curve on dates from Lake Immeln, Sweden, Digerfeldt (1974) obtained a good agreement between observed and predicted ages.

Where a very large number of radiocarbon dates are available it should be acceptable to employ statistically more complex curve-fitting techniques. On the other hand, such close dating also better enables the fitting of a subjective curve expressing the 'general relationship' between the sample depth and age (e.g. Davis, 1969). Alternatively, a simple curve smoothing technique such as the calculation of a running mean for five consecutive dates, may be employed. Aaby and Tauber (1975) used this method to reconstruct rates of peat formation at Draved Mose, Denmark, as they did not wish to make the assumption of a linear accumulation rate presupposed by the use of a straight line regression. Where a substantial number of dates indicates a fairly smooth curve,

there may be, as Kendall (1969) suggests, 'no apparent or statistical method more accurate than simply connecting the ^{14}C points... with straight lines'.

Estimation of sediment accumulation rates for core LW II

Examination of both the age/depth curve based on the reported radiocarbon dates, and on the recalibrated dates (Fig. 3.10) leads to the conclusion that no simple linear relationship exists between depth and age. Neither can the fluctuations in the average sediment accumulation rate (Table 3.3) be explained by autocompaction of the deposits alone. Although the accumulation is considerably lower towards the base of the core (dating intervals I-L) the sediment density profiles (Fig. 3.9) do not show a corresponding degree of increase during this time. Furthermore, the periods of most rapid apparent accumulation occur in the middle sections of the core, not towards the top as would be the case were a constant deposition rate modified only by compaction to be postulated.

It is therefore concluded that measurable change in the real accumulation rate has been operative during the time-scale represented by the core. Consequently it does not seem appropriate to derive an annual accumulation curve by fitting a simple regression model to the age/depth curve. Lack of sufficient replicated samples precludes analysis of the age/depth results using more sophisticated, non-linear statistical techniques.

A first approximation (Accumulation Rate 'A') of the annual accumulation rate (Fig. 3.11a) was therefore derived from the figures in Table 3.3. This represents the average rate of

FIGURE 3.11. Lake Wanum core LW II: Average sediment accumulation rates

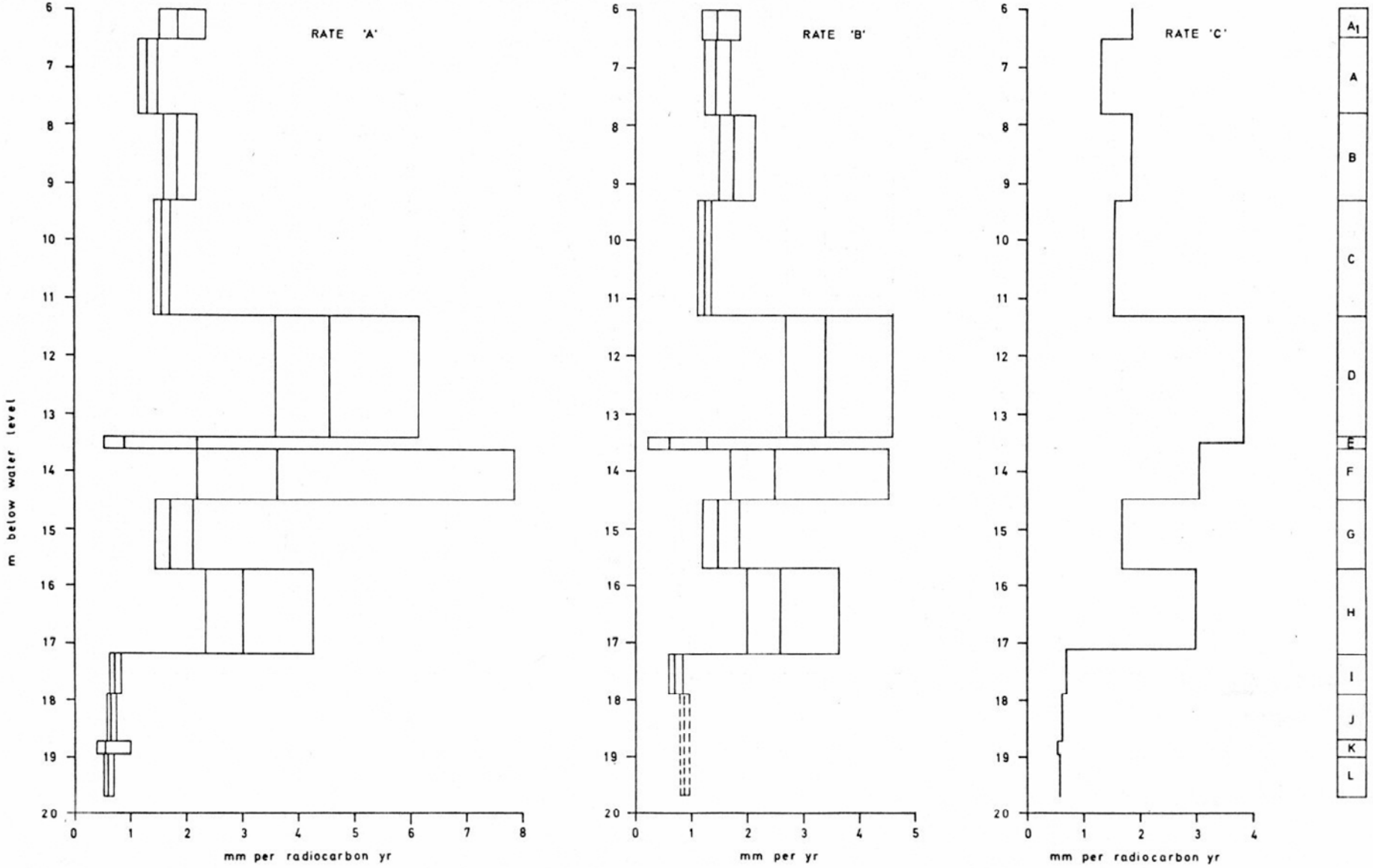

apparent annual sediment accumulation, disregarding autocompaction, between pairs of radiocarbon dates. A curve produced in a similar fashion from the recalibrated dates (Accumulation Rate 'B') is shown in Fig. 3.11b. The values for minimum and maximum average rates are based on plus or minus one standard deviation of the interval between dates. This represents an overestimation as the calculation method treats each pair of dates as independent from the adjacent pairs, which is obviously not the case. It must be emphasised that the maximum and minimum limit is based only on the size of the combined radiocarbon counting errors, in relation to the length of the time interval between dates. It therefore applies only to the *average* accumulation rate and gives no direct indication of the amplitude and frequency of fluctuations around this mean. It may be reasonable to suppose that where consecutive average values are similar, fluctuations around these are generally similar also. Conversely, where averages for adjacent dating intervals are very dissimilar, this may be caused by differences in the amplitude and/or frequency of fluctuations in the accumulation rate.

A curve better representative of the actual accumulation rate needs to take into account

(a) the statistical significance of the individual radiocarbon dates and of the intervals between dates, and

(b) any evidence in the stratigraphy of discontinuities in the deposits, or abrupt changes to the rate of sediment accumulation.

Although the general sequence of dates appears valid, several of the paired ages are close in relation to their counting errors. In particular, the estimated duration of intervals E and F is less than twice the standard deviation of each interval. Using

the criteria of Polach and Golson (1966) it is thus 'fairly probable' that the two age determinations defining each interval differ with statistical significance, but the exact interval between them cannot be estimated with accuracy.

The horizon encompassed by interval E is a well defined grey clay (*As*) band which possibly represents a slight unconformity, due to erosion of earlier sediment, or cessation of organic sedimentation. Lacking clear evidence, an accumulation rate for this interval is assumed that is not too dissimilar from the adjacent periods. A mean of the two dates ANU-1447 and ANU-1446 was therefore taken. Average accumulation rates were then calculated for two intervals, DE and EF, instead of three, becoming 3.85 mm yr^{-1} and 3.07 mm yr^{-1} respectively. This procedure serves to increase the timespan of each interval in relation to its standard deviation and also reduces the fluctuation in the average accumulation rate.

All other dating intervals are of comparatively long duration in relation to their error terms, and may therefore be taken as statistically well defined.

At two boundaries C/DE, and H/I, a change in the accumulation rate by an order of magnitude appears to be indicated. Only one of these shows a concurrent indication in the stratigraphy that might be associated with such a major change in sediment accumulation. The fourfold increase in the rate between intervals H and I appears to be marked by an horizon of gritty orange-grey clay (*Ga* + *As*) with a sharp upper boundary. This horizon produces the greatest peak on the inorganic sediment density curve (Fig. 3.9). Although an unconformity in the sequence during interval I is

possible, this seems unlikely given the concordance of accumulation rates between this and the underlying periods. As the gritty clay penetrates well into the I interval, it seems more reasonable to propose a rapid increase in accumulation subsequent to this stratum, although the clay may reflect initiation of the change. The sediment analysis sample taken from 1710 to 1711 cm that includes a proportion of the clay band, was regarded as having an accumulation rate intermediate between that of intervals H and I.

A grey clay band (*As*) in interval G may also be responsible for a slight discontinuity in accumulation around 1487 to 1488 cm. This may account for the lower average accumulation rate for this period. However, no correction has been attempted.

Stratigraphic evidence for abrupt changes in the accumulation rate at the C/DE boundary is lacking. Theoretically, a 'smoother' curve would probably represent a better approximation of the actual accumulation rate at this boundary. Any such modification of the curve would however have to be extreme to affect the widely spaced samples in this section of the core. Given the acceptable radiocarbon dates, major modification was considered inappropriate, and no correction has been applied.

The average annual sediment accumulation curve, incorporating the modifications described above, is shown in Fig. 3.11c. The average accumulation rate of wet sediment for any part of the core may be read from this curve. Any sample occurring at a boundary between dating intervals is assumed to have an accumulation rate intermediate between the two.

Gravimetric estimates of annual sediment deposition

By applying the corrections for the average annual sediment accumulation rates to the figures for density[1] (mg dry weight ml^{-1}) of organic and inorganic sediment (Fig. 3.9) an estimate of annual gravimetric deposition rate for these sediment fractions may be obtained. Such estimates are shown assuming accumulation rate 'A' (Fig. 3.12) and accumulation rate 'C' (Fig. 3.13).

The main differences between the estimates based on the two accumulation rates are in the values for the inorganic sediment fraction. This curve is characterised by sharp peaks that probably represent depositional phases of short duration in relation to the dating interval in which they occur. Applying accumulation rate 'A', the highest value for inorganic deposition is found in the sample from 1710 to 1711 cm. Using the modified rate 'C', this value decreases, and the distinct clay band at 1346 to 1348 cm gives the largest peak. With the current method of dating it is impossible to resolve accurately the absolute annual deposition rate, or even the relative deposition rate for such sedimentary episodes.

As the mean value for organic sediment density (Fig. 3.9b) remains essentially similar throughout the core, variation in the annual deposition rate is very largely a product of the correction for average accumulation rate. Thus the major difference reflected in the curves derived from the two accumulation rates is in the middle section of the core. Here the higher accumulation rates suggested by rate 'A' are reflected in increased organic deposition also.

---

[1] i.e. bulk density

FIGURE 3.12. Lake Wanum core LW II: Gravimetric sediment deposition rates based on accumulation rate 'A'

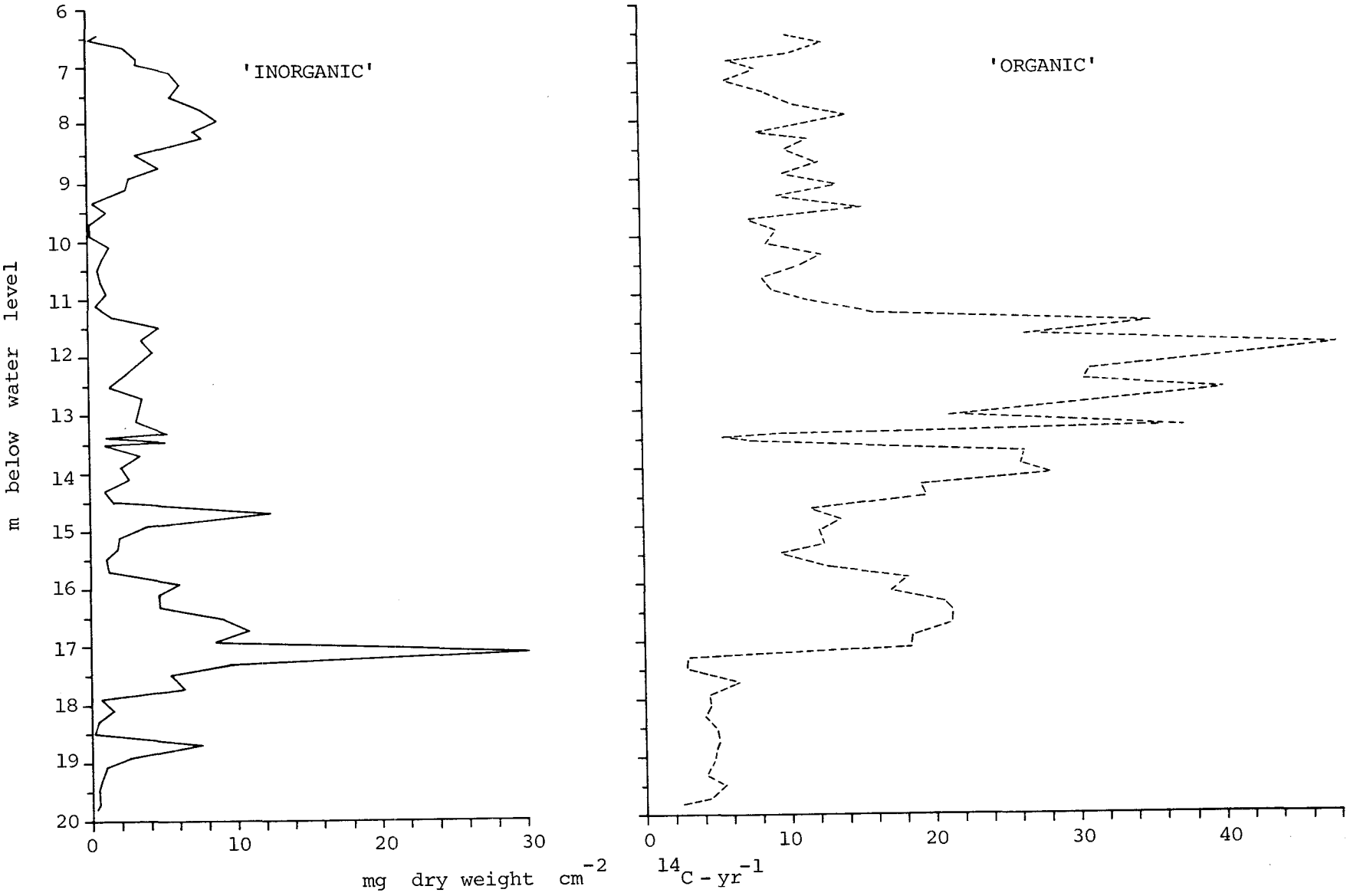

FIGURE 3.13. Lake Wanum core LW II: Gravimetric sediment deposition rates based on accumulation rate 'C'

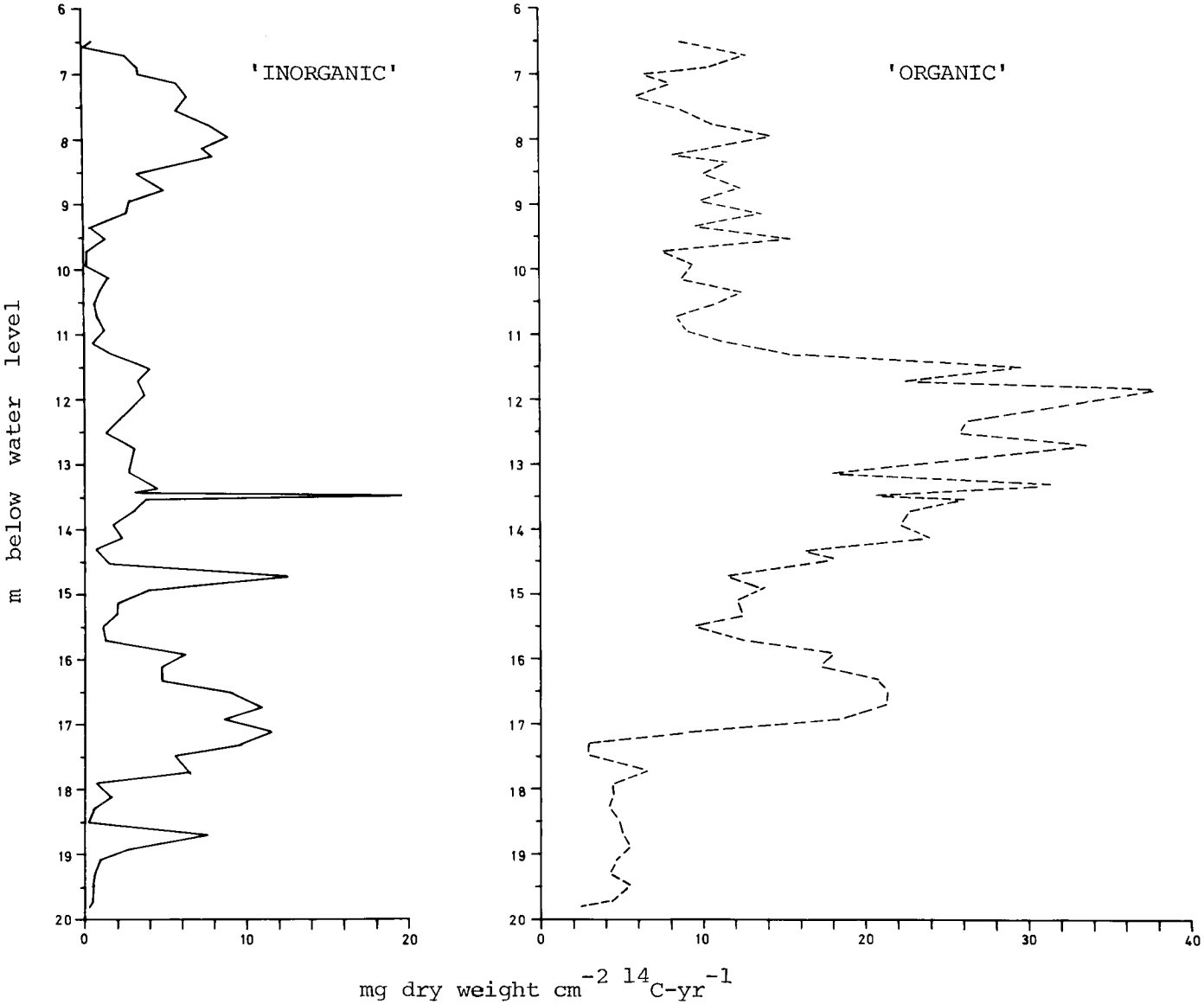

SUMMARY OF MAJOR TRENDS IN THE SEDIMENTATION OF CORE LW II

The main trends in the average sediment accumulation rates and annual gravimetric deposition rates in core LW II may be summarised by dividing the sequence into three zones as follows.

(1) From the base of the core at about 9500 BP until *c.* 5500 BP (6300 years corrected age).

(2) A period following this of about 2000 years until approximately 3400 BP.

(3) The uppermost part of the core representing deposits from about 3400 BP to the present.

The lowest zone exhibits a low but fairly constant average sediment accumulation rate of between 0.5 mm yr^{-1} and 1.0 mm yr^{-1}. Although the deposits are predominantly organic two peaks occur in the inorganic deposition rate. These are produced by horizons containing gritty orange-grey clay (*Ga* + *As*) rather than the plastic grey clay (*As*) more common above.

The middle zone possesses the most rapid accumulation rate and the highest values for both organic and inorganic fractions. A number of phases of grey clay sedimentation occur within the predominantly organic matrix. The most intense of these appear to be of short duration. This zone also displays the largest apparent fluctuations in accumulation rate.

In the uppermost zone, the average accumulation rate appears to stabilise at between 1 mm yr^{-1} to 2 mm yr^{-1}. Although the sediment is mainly organic without discrete clay bands, there is a gradual increase in inorganic sedimentation rising to a peak at about 1300 BP, and thence declining towards the top of the core.

This three-zone generalisation may be the most appropriate level of resolution at which to review the accumulation and deposition rates from the core. Stratigraphic corroboration for

gross changes in the accumulation rate is generally lacking. Certainly, the changes apparently represented in the central section of the core must be interpreted with circumspection, this being the period both of greatest fluctuation in sediment accumulation, and of the most rapid sustained change in atmospheric radiocarbon concentration yet demonstrated.

COMPARISONS WITH OTHER CORES

Although there are few horizons in the other cores from Lake Wanum that can be correlated either by radiocarbon dates or stratigraphic markers, it is possible to derive gross accumulation rates for several other cores.

Within the western part of the north-east bay, cores LW II and LW 6 possess closely similar average accumulation rates (1.46 mm yr^{-1} and 1.48 mm yr^{-1} respectively) for their total periods of sedimentation. During about 4000 BP to the present, core LWA 1 appears to record a slightly higher accumulation rate than LW II, although this could be explained by lack of recovery of the uppermost highly unconsolidated material. LWA 4 also shows a similar, or perhaps slightly higher accumulation rate than LW II for this period.

The most rapid accumulation rate for any period is shown by the upper section of core LW I. Here the interval between a date of 2070 BP and the present is represented by 955 cm of loosely compacted fibrous organic deposit (*Th*) giving an average accumulation rate of 4.6 mm yr^{-1}. This figure is more analogous to the highest estimate for the accumulation rate of dating interval D in core LW II than with the synchronous deposits from the latter core.

Extrapolation of possible accumulation rates to the south swamp suggests an accumulation time of perhaps only two to six years for the thin cover of organic deposit in that area.

Such comparisons indicate that the sedimentation results from core LW II may be representative of more general conditions in the western part of the north-east bay. Although the range of deposits found in the cores from the central area of the bay is similar there are differences in the stratigraphy and accumulation rates by comparison with the cores from the western margin of the bay. This divergence could be explained by the presence of dry land between the two coring areas. Given a lower water level, this is quite feasible, as solid ground occurs under less than 1 m of water about 50 m south-west of LW I coring site. The possibility of a less continuous water surface must therefore be taken into account when attempting to interpret the results from core LW II in terms of events in the Lake Wanum basin as a whole.